Journal of Catalysis **210,** 445–452 (2002)
doi:10.1006/jcat.2002.3700

Molecular Competition of C_7 and C_9 *n*-Alkanes in Vapor- and Liquid-Phase Hydroconversion over Bifunctional Pt–USY Zeolite Catalysts

Joeri F. M. Denayer,*,[1] Bruno De Jonckheere,† Myriam Hloch,† Guy B. Marin,‡ Gina Vanbutsele,† Johan A. Martens,† and Gino V. Baron*

*Dienst Chemische Ingenieurstechniek, Vrije Universiteit Brussel, Pleinlaan 2, B-1050 Brussels, Belgium; †Centrum voor Oppervlaktechemie en Katalyse, Katholieke Universiteit Leuven, Kasteelpark Arenberg 23, B-3001 Louvain, Belgium; and ‡Laboratorium voor Petrochemische Techniek, Universiteit Gent, Krijgslaan 281, B-9000 Ghent, Belgium

Received March 14, 2002; revised May 28, 2002; accepted May 28, 2002

Molecular competition effects in the hydroconversion of an equimolar heptane/nonane mixture were studied in liquid-phase reaction conditions in a fixed-bed reactor filled with a Pt–ultrastable-Y (USY) catalyst. Liquid-phase conditions were attained by feeding the hydrocarbon mixture with hydrogen dissolved in it at 100 bar and 230°C. Comparative vapor-phase experiments were run at 230°C, a pressure of 4.5 bar, and a hydrogen-to-hydrocarbon ratio of 13. Whereas catalytic experiments in the vapor-phase showed a marked referential conversion of nonane over heptane, in liquid-phase the differences in conversion rate between nonane and heptane were much less pronounced. Adsorption-reaction models were used to explain the difference. For this purpose, intrinsic kinetic constants for heptane and nonane were derived from experimental data from vapor-phase conversions of the *n*-alkanes individually, using an adsorption-reaction model with independently determined adsorption equilibria, and assuming the classic bifunctional reaction scheme. The liquid-phase conversion of the heptane/nonane mixture was predicted very well using these intrinsic reaction kinetics derived from the vapor-phase experiments and assuming no adsorption preference between heptane and nonane. In contrast to this, the conversion of the heptane/nonane mixture in the vapor phase could only be appropriately described by a model involving adsorption according to a Langmuir-with-interaction model, favoring adsorption of the heaviest compound. In liquid-phase reaction conditions and at saturation of the Pt–USY zeolite pores with *n*-alkanes, there is no such selective adsorption of the heaviest compound. In liquid-phase, the conversion of the mixture reflects the intrinsic reaction kinetics of the individual compounds.

Key Words: **hydrocracking; alkane; Pt/USY zeolite; liquid phase; kinetic modeling.**

INTRODUCTION

Bifunctional zeolite catalysts are applied in several petroleum refinery operations, designated as hydroconversion processes. The most important zeolite-based petrochemical hydroconversion processes are isomerization of light naphtha, iso-dewaxing, and hydrocracking of heavy fractions (1). The hydroconversion of hydrocarbon molecules on platinum-loaded acid zeolite catalysts is an appealing research subject in view of these important industrial applications. Experimental investigations in academic laboratories are typically performed with pure model components or simple mixtures thereof as feedstock, and under reaction conditions where the hydrocarbon compounds are in the vapor phase. (2–5). Industrial hydroconversion processes are mostly run under three-phase, or even in some cases under liquid-phase conditions and with feedstocks that are extremely complex mixtures of large numbers of different hydrocarbon compounds (1).

At the relatively mild reaction temperatures relevant to these hydroconversion processes, even under vapor-phase reaction conditions, the zeolite pores are filled with physisorbed molecules to a significant extent. In earlier work, adsorption equilibria of a broad range of hydrocarbon components were determined on ultrastable-Y (USY) zeolites under catalytic conditions. It was found that Henry adsorption constants increase exponentially with the alkane carbon number (6, 7). This adsorptive discrimination of long alkanes in favor of shorter alkanes is most pronounced in the Henry regime and decreases when the pores are more filled with hydrocarbon molecules at increasing vapor pressures (8). USY-type zeolite contacted with liquid alkanes does not show any difference in affinity toward alkanes of different molecular weight (9). These investigations showed that on USY-type zeolite, adsorption selectivity depends strongly on the loading of the micropores and on the aggregation state of the alkane contacted with the zeolite. In contrast to the vast amount of literature dealing with hydroconversion processes of model compounds in the vapor-phase, only very few experimental studies dealing with liquid-phase reaction conditions have been reported (10, 11).

Reaction pathways of bifunctional catalytic conversions of model hydrocarbon compounds were experimentally

[1] To whom correspondence should be addressed. Fax: +32 2 6293248. E-mail: Joeri.Denayer@vub.ac.be.

0021-9517/02 $35.00

determined and explained in terms of rearrangements and scissions of alkylcarbenium ions (12, 13). The alkylcarbenium ions are obtained through dehydrogenation on a noble metal particle and protonation on a zeolite Brønsted acid site (14). The conversions of *n*-alkanes, cycloalkanes, and their mixtures over Pt–USY zeolites under vapor-phase reaction were successfully modeled using independently determined adsorption equilibria and fundamental reaction networks based on alkylcarbenium ion chemistry (15–18). In these models, the intrinsic reaction rate of an individual reaction step such as a branching rearrangement via a protonated cyclopropane is the same in all molecules and at all positions in the carbon chain. Intrinsic reactivity differences between alkene intermediates are accounted for by one single parameter, reflecting differences in protonation enthalpy (16). The model adequately described the hydroconversion of a quaternary mixture of *n*-alkanes at about 70% saturation of the adsorption capacity of the Pt–USY zeolite.

In the different hydroconversion applications, governing the relative reactivity of the different components of the feed is extremely important. Under vapor-phase reaction conditions on a Pt–USY-type catalyst, there is always preferential conversion of the heaviest alkane due to its preferential adsorption (2, 3). The aim of this study was to investigate whether operation of the reactor in the liquid instead of the vapor phase would enhance the reactivity of the lighter compounds as expected, based on earlier sorption studies (9). For this purpose, an equimolar mixture of heptane and nonane was converted on a Pt–USY catalyst in both liquid- and vapor-phase conditions. In absence of adsorption selectivity in the liquid phase, it is expected that the relative reactivities of the two hydrocarbons reflect the intrinsic reaction kinetics of vapor-phase experiments.

EXPERIMENTAL

Materials

The dealuminated Y zeolite CBV720 (Si/Al = 13, Zeolyst) was loaded with 0.5 wt% platinum by incipient wetness impregnation with aqueous $Pt(NH_3)_4Cl_2$ solution. The zeolite powder was compressed into a solid disc, crushed, and sieved and the 300–500 μm pellet fraction was retained for the catalytic experiments. The catalyst activation procedure comprised calcination under flowing oxygen at 400°C followed by reduction in hydrogen at the same temperature.

Catalytic Experiments

Data for the conversion of pure nonane were retrieved from earlier work (18). Catalytic experiments were performed with heptane and an equimolar mixture of both heptane and nonane (99% purity, Acros). In the vapor-phase experiments, the total pressure in the reactor was 4.5 bar and the temperature was 230°C. The hydrogen-to-hydrocarbon molar ratio in the feed was 13. Contact times were up to 800 kg s/mol. The hydrocarbon was fed by an HPLC pump from a reservoir into a vaporization chamber, mixed with hydrogen, and passed in downflow direction over the fixed catalyst bed, held in a tubular reactor. Analysis of the reaction products was done online using capillary GC, splitless cool-on-column injection using a six-way sampling valve with external sampling loop, and temperature programming from 10 to 114°C.

The liquid-phase catalytic experiments were performed in a different reactor. A feedstock storage vessel was filled with an equimolar mixture of heptane and nonane, flushed with nitrogen, and pressurized at 100 bar with hydrogen. The hydrogen pressure on the storage vessel was kept constant throughout the experiment. The amount of hydrogen dissolved in the liquid hydrocarbon mixture was determined volumetrically and corresponded to a hydrogen-to-hydrocarbon molar ratio of 0.5. Liquid-phase conditions were guaranteed at the reaction temperature of 230°C and the pressure of 100 bar in the reactor. The flow of the hydrocarbon liquid containing dissolved hydrogen was controlled by a liquid mass flow controller. The contact time in the liquid-phase experiments was between 100 and 500 kg s/mol. Samples of the reactor effluent were analyzed online by capillary GC using a four-way sampling valve with small internal sample volume of 1 μl. Otherwise the same procedures were followed as in the vapor-phase experiments.

RESULTS AND DISCUSSION

Vapor-Phase Experiments

Vapor-phase experiments with pure heptane and nonane feeds were conducted to determine intrinsic reaction constants and to compare the molecular competition in the vapor phase with the liquid-phase. The conversion of heptane and of nonane in separate vapor-phase catalytic experiments using the Pt–USY catalyst is plotted against space-time in Fig. 1. Nonane was more reactive than heptane, in agreement with previous investigations (15). The selectivity for formation of monobranched (MB) and multibranched (MTB) isomers and cracked reaction products from heptane and nonane is shown in Figs. 2 and 3, respectively. Both linear alkanes are initially transformed into their monobranched isomers, which undergo additional branching and cracking. MB and MTB isomers of the *n*-alkane, and cracked products (CRs) are formed in consecutive steps (12) according to the following reaction scheme (12, 19):

$$n\text{-alkane} \overset{k_{MB}}{\rightleftarrows} \text{MB} \overset{k_{MTB}}{\rightleftarrows} \text{MTB} \xrightarrow{k_{CR}} \text{CR}. \qquad [1]$$

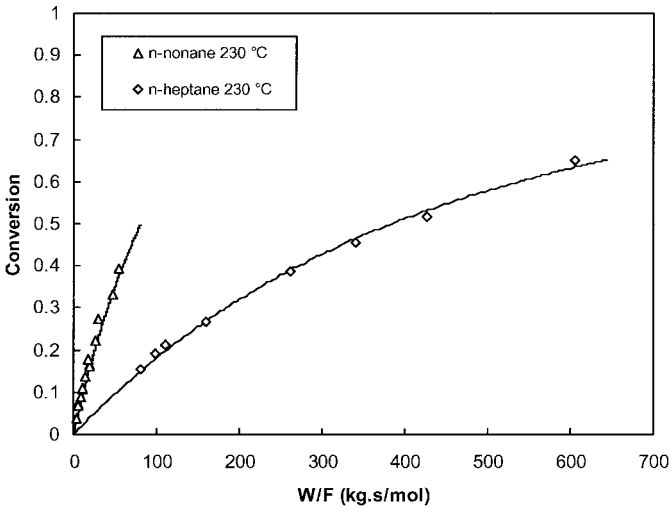

FIG. 1. Conversion of nonane and heptane in separate experiments in vapor-phase conditions on Pt–USY catalyst at 230°C.

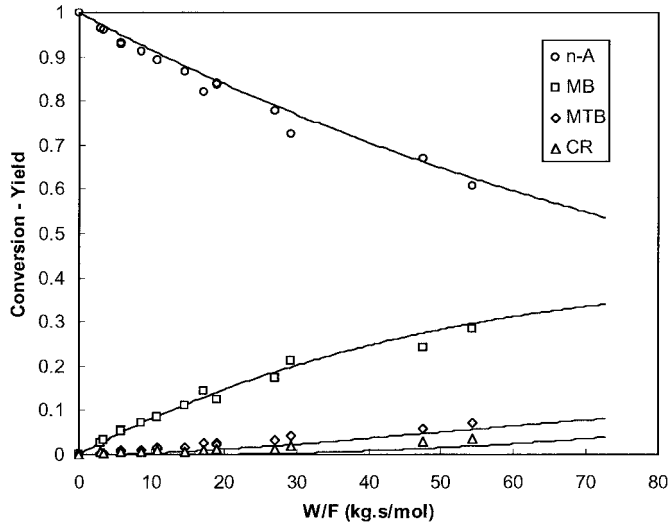

FIG. 3. Yield of nonane, MB isononanes, MTB isononanes, and CR from nonane conversion on Pt–USY at 230°C in vapor-phase reaction conditions (experiment from Fig. 1).

The experimental conversion data for the individual components of an equimolar mixture of heptane and nonane at various space-times with the catalyst bed are shown in Fig. 4. In the mixture, nonane is much more reactive than heptane. The product distributions from nonane and heptane conversion in the experiment with mixed feed were very similar to those obtained in the experiments with the two *n*-alkanes individually, confirming that the reaction networks of these two molecules are independent (20).

Liquid-Phase Experiments

The conversion of the equimolar *n*-alkane mixture in the liquid phase at 100 bar and 230°C and different space-times is reported in Fig. 5. In the experiments in liquid phase, the yield patterns of MB isomers, MTB isomers and CRs were similar to those in the vapor-phase experiments. In contrast to the vapor-phase conditions where the catalyst did not show any deactivation, in the liquid-phase experiments with the low hydrogen/hydrocarbon ratio of 0.5, the catalyst was stable only under conditions where there was no hydrocracking. Attempts to reach conversion levels exceeding 50% by increasing the contact time failed and led to catalyst deactivation.

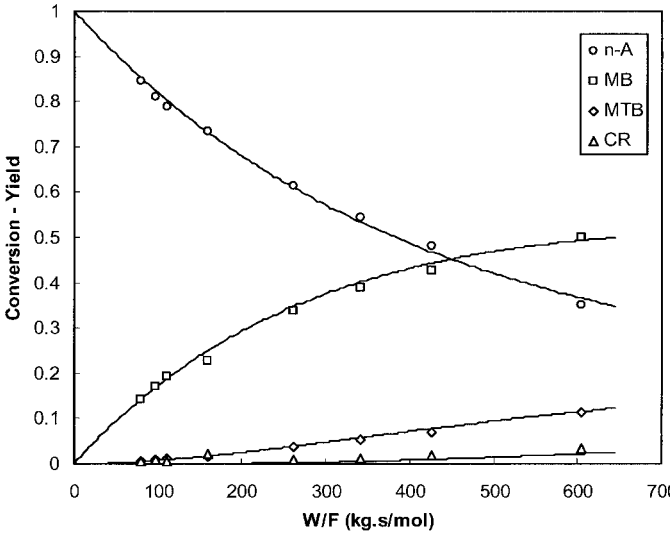

FIG. 2. Yield of heptane, MB isoheptanes, MTB isoheptanes, and cracked products (CR) from heptane conversion on Pt–USY at 230°C (experiment from Fig. 1).

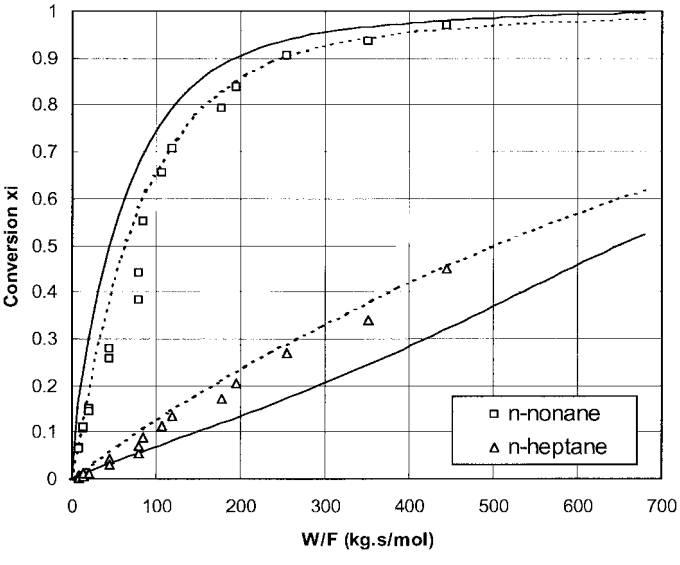

FIG. 4. Conversion of heptane and nonane from their binary equimolar mixture in vapor-phase conditions at 230°C and different space-times: symbols, experimental data points; solid curves, Langmuir adsorption model; dotted curves, Langmuir-with-interaction model.

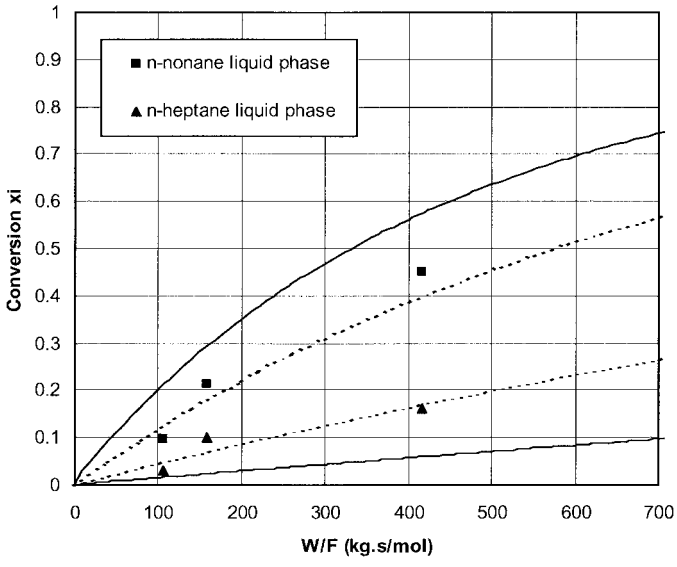

FIG. 5. Conversion of heptane and nonane from their binary equimolar mixture in liquid phase at 230°C and at different space-times: symbols, experimental data points; solid curves, Langmuir adsorption model; dotted curves, no selective adsorption.

The observed reaction rates in liquid phase were lower than in vapor phase (Fig. 6). This can be explained by the higher concentration of dissolved hydrogen in the zeolite pores compared to the vapor-phase experiments, which shifts the dehydrogenation equilibrium to a lower alkene concentration (see Eq. [12]). One could expect a lower deactivation rate in liquid phase as a consequence of this lower alkene concentration, but this was not observed experimentally. In the liquid-phase experiments, the hydrogen-to-hydrocarbon molar ratio is only 0.5, whereas it is 13 in the vapor-phase experiments, although the total hydrogen pressure is lower in the vapor-phase experiments. With increasing degree of conversion, hydrocracking becomes more important. In the hydrocracking reaction, an alkylcarbenium ion is cracked into a smaller alkylcarbenium ion and an alkene fragment. The alkylcarbenium ion is deprotonated into a second alkene molecule. Thus, two alkene molecules have to be hydrogenated into alkanes, resulting in a global consumption of one hydrogen molecule per cracked alkane molecule. In the vapor-phase experiments, there is large excess of hydrogen compared to alkane, hence alkenes formed during cracking reactions can always be hydrogenated into alkanes. In contrast, in liquid phase the hydrogen is rapidly depleted when hydrocracking reactions occur, since the hydrogen-to-hydrocarbon ratio is only 0.5. Consequently, at higher conversions, hydrocracking reactions result in a formation of alkenes, which polymerize and deactivate the catalyst. The conversion data from Fig. 5 are presented against the average conversion in Fig. 7 Experimental data points obtained with partially deactivated catalyst were included. Data on fresh and deactivated catalyst lie on the same curve. Apparently, deactivation did not alter the competition between the two molecules. In the integral reactor and according to the reaction scheme [4], deactivation associated with hydrogen consumption through hydrocracking is expected to affect a bottom part of the packed catalyst bed only.

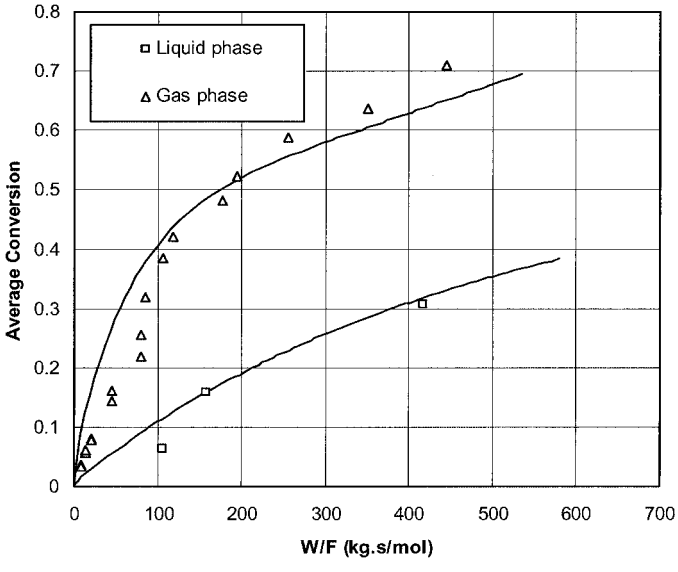

FIG. 6. Average conversion of the heptane/nonane equimolar mixture against space-time in vapor- and liquid-phase reaction conditions: symbols, experimental data; lines, theoretical curves.

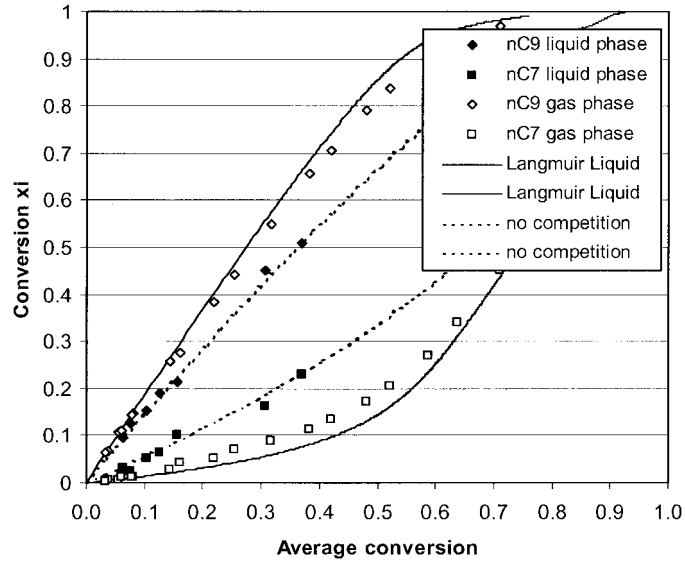

FIG. 7. Conversion of heptane and nonane from their binary mixture in liquid phase plotted against the average conversion: symbols, experimental data points; solid curves, Langmuir adsorption model; dotted curves, no selective adsorption.

TABLE 1

Molecular Competition Factor ζ of Nonane Versus Heptane Hydroconversion

	Vapor phase		Liquid phase
	Pure compounds	Mixture	Mixture
Experimental	4.3	8.4	2.7
Kinetic model with competitive adsorption			
Langmuir	—	16.9	13.9
Langmuir-with-interaction	—	8.9	—
No competition	—	—	2.6

Expression of Molecular Competition

To quantify the competition effects between nonane and heptane, a molecular competition factor ζ was introduced:

$$\zeta = \frac{r^0_{n\mathrm{C9}}}{r^0_{n\mathrm{C7}}} \qquad [2]$$

where r^0 denotes the observed initial reaction rate derived from the slope of conversion versus contact time curves below 20% conversion. This ratio of apparent reaction rates reflects the relative adsorption of the two *n*-alkanes, the dehydrogenation equilibria, and intrinsic kinetics of *n*-alkene into branched alkene conversions. Based on the apparent reaction rates of nonane and heptane converted separately in vapor-phase conditions, ζ equals 4.3 (Table 1, first row). When both components are contacted with the catalyst in an equimolar mixture, ζ is equal to 8.4 (Table 1). In the mixture in vapor phase, the relative conversion rate of nonane compared to heptane is thus almost twice as high as expected from experiments with individual compounds. In the liquid phase, the ζ factor amounts to only 2.7 (Table 1), which shows that the reactivities of nonane and heptane are much more similar.

Adsorption Model for Vapor-Phase Conditions

Perturbation chromatography experiments with Y zeolites indicate that the preferential adsorption of a long *n*-alkane at the expense of a shorter *n*-alkane is most pronounced in the Henry region, where interactions between the adsorbed molecules are absent (6). The differences in adsorbed amounts of two competing alkanes decrease at higher loading of the zeolite with adsorbate. For instance, on a Y zeolite with a Si/Al ratio of 2.7, a steep drop in competition was observed at a loading corresponding to one molecule per supercage (8). This observation can be explained in two ways. There may be significant changes in adsorption enthalpy with loading due to surface heterogeneity or mutual interactions between adsorbed molecules. Further, there may be entropy changes due to a change of adsorbate mobility when the cages of the zeolite are filled with molecules.

An adequate theoretical model accounting for this loading dependence of the competitive sorption equilibrium on Y zeolites is not available. In this work, two types of adsorption isotherms were used: the Langmuir isotherm (Eq. [3]), and an extended form of the Langmuir isotherm, which is denoted here as the Langmuir-with-interaction isotherm (Eq. [4]). The multicomponent Langmuir isotherm assumes that the competition between different molecules is independent of the loading of the adsorbent with molecules (21). This model does not account for the experimentally observed decrease in selective sorption between long- and short-chain alkanes with increasing zeolite loading (8). The Langmuir-with-interaction isotherm contains an additional term which accounts for a loading dependent competition.

$$\text{Langmuir:}\quad q_i(p,T) = \frac{K'_i p_i}{1+\sum_j L_j p_j} \qquad [3]$$

$$\text{Langmuir-with-interaction:}\quad q_i(p,T) = \frac{K'_i p_j e^{w_i \frac{q_\mathrm{T}}{\bar{q}_\mathrm{s}}}}{1+\sum_j L_j p_j e^{w_j \frac{q_\mathrm{T}}{\bar{q}_\mathrm{s}}}} \qquad [4]$$

q_i represents the amount of alkane i adsorbed from the reaction mixture. The denominator accounts for adsorption of all alkanes (reactants: *n*-alkanes, intermediates: mono- and multibranched alkanes, products: cracked alkanes). Since the amount of olefins is kept very low due to the unfavorable dehydrogenation equilibrium, their adsorption is not taken into account.

In the Langmuir-with-interaction model, q_T represents the total amount adsorbed, and $\bar{q}_\mathrm{s}$ the mean saturation capacity for the n compounds considered, defined as

$$\bar{q}_\mathrm{s} = \frac{1}{n}\sum_{i=1}^{n} q_{i,\mathrm{s}}. \qquad [5]$$

Adsorption Model for Liquid-Phase Conditions

For the liquid-phase conditions, the isotherms are written in terms of concentrations instead of gas-phase partial pressures. In a first approach, the Langmuir isotherm is expressed as

$$q_i(c,T) = \frac{K^\mathrm{L}_i c_i}{1+\sum_j L^\mathrm{L}_j c_j} \qquad [6]$$

with

$$K^\mathrm{L}_i = K'_i RT V_\mathrm{m} \qquad [7]$$

and

$$L^\mathrm{L}_j = \frac{K^\mathrm{L}_j}{\bar{q}_\mathrm{s}}. \qquad [8]$$

The saturation adsorption capacity used here is the same as that used for the vapor-phase modeling. This Langmuir

liquid-phase multicomponent model predicts the same molecular competition as the gas-phase Langmuir model.

In a second approach, the adsorption in liquid phase is represented by a partition coefficient model,

$$q_i = K_i c_i. \quad [9]$$

Liquid-phase chromatographic adsorption experiments showed that the partition coefficients of alkanes are all equal (9):

$$K_i = \bar{q}_s V_m. \quad [10]$$

The latter model for liquid-phase adsorption thus implies that no selective enrichment of a particular alkane occurs.

Adsorption-Reaction Models

According to the bifunctional reaction mechanism [1], *n*-alkanes are dehydrogenated to alkenes on platinum. The alkene concentration is calculated from the hydrogenation/dehydrogenation equilibrium. For the vapor phase experiments this gives

$$q_O = \frac{K_{DH}^{vap} q_A}{p_{H_2}} \quad [11]$$

For the liquid-phase conditions, the following equation is used (22):

$$q_O = \frac{K_{DH}^{vap} q_A}{C_{H_2}^L \phi_{H_2}^L P V_m}. \quad [12]$$

n-Alkenes are protonated on the Brønsted acid sites of the zeolite into alkylcarbenium ions, which are isomerized and cracked. Assuming that (i) the rate-limiting steps in the reaction scheme are the rearrangement and cracking reactions of alkylcarbenium ions (14), (ii) the concentration of chemisorbed carbenium ions is negligible compared to the total number of active sites (19), and (iii) the adsorption and desorption and (de)hydrogenation steps are in quasi-equilibrium, the following rate equations are obtained:

$$r_{alkane,i} = k_{MB,i}\left(q_{nO,i} - \frac{q_{MBO,i}}{K_{MB,i}}\right), \quad [13]$$

$$r_{MB,i} = \left[k_{MB,i}\left(q_{nO,i} - \frac{q_{MBO,i}}{K_{MB,i}}\right) - k_{MTB,i}\left(q_{MBO,i} - \frac{q_{MTBO,i}}{K_{MTB,i}}\right)\right], \quad [14]$$

$$r_{MTB,i} = k_{MTB,i}\left(q_{MBO,i} - \frac{q_{MTBO,i}}{K_{MTB,i}}\right) - k_{CR,i} q_{MTBO,i}, \quad [15]$$

$$r_{CR,i} = k_{CR,i} q_{MTBO,i}. \quad [16]$$

The experimental catalytic data were modeled with a kinetic model that accounted for competitive adsorption in the zeolite micropores of the reactants (the *n*-alkanes) and the products (MB and MTB isoalkanes and CRs). For the vapor-phase conditions, the relationship between external pressure of a specific component from a mixture and its amount adsorbed in the pores is expressed by a Langmuir or Langmuir-with-interaction multicomponent adsorption isotherm (Eqs. [3] and [4]). For the modeling of the liquid-phase experiments, equations [6]–[10] are used.

TABLE 2

Intrinsic Kinetic Constants for Monobranching, Multibranching, and Cracking of Heptane and Nonane on Pt–USY at 230°C Obtained from Vapor-Phase Experiments and Fitting with the Model

Rate constant	C_7	C_9
k_{MB} (1/s)	2900	8100
k_{MTB} (1/s)	1300	6500
k_{CR} (1/s)	1000	3700

The rate equations [13]–[16] were solved with a fourth-order Runge–Kutta algorithm and fitted to the experimental pure component conversion data using a quasi-Newton method. Vapor-phase adsorption constants for heptane and nonane and their branched isomers on the particular USY sample were retrieved from earlier work (6) and used in fitting the model with the experimental data obtained with the single feeds (Fig. 1). This approach yielded estimated values for the kinetic constants (Table 2). The kinetic constants for pure heptane reported here differ slightly from those obtained in earlier work that modeled the conversion of a quaternary feed containing heptane (15), which is not unexpected since competitive adsorption effects in mixtures lead to an inaccurate determination of the kinetic constants.

The relative values are as expected from a more fundamental model for hydrocracking and are in particular in line with the higher number of possible alkylcarbenium ion transformations for nonane (17). The kinetic constants reported in Table 2 were used later to model the conversion of the binary mixture in vapor and liquid phase.

Experimental data were not available on the multicomponent adsorption equilibrium on the USY zeolite sample used in this work at the loading relevant for the vapor-phase experiments (ca. 85% of the zeolite saturation capacity). The interaction parameter w (Eq. [4]) was estimated by fitting the experimental data from the catalytic vapor-phase experiments with the mixed feed with the model (Table 3). A satisfactory fitting was obtained using the multicomponent Langmuir-with-interaction isotherm, as shown by the curves in Fig. 4. According to the multicomponent Langmuir-with-interaction isotherm expression, under the experimental conditions with the mixed feed in the vapor phase, the nonane concentration in the pores was 2.2 times that of heptane. According to the multicomponent Langmuir expression without the interaction term, the

TABLE 3

Henry and Langmuir Adsorption Constants and Interaction Parameters for Competitive Adsorption of Nonane and Heptane on Pt–USY at 230°C[a]

Parameters	Nonane	Heptane
K (mol/kg/bar)	37.4	6.91
L (1/bar)	59.96	9.80
w	−0.77	0.3

[a] Data from (6, 8).

adsorbed nonane concentration is 5.4 times that of heptane. This significant difference illustrates the importance of the interaction term.

The model involving the multicomponent Langmuir adsorption isotherm predicts the average conversion of the mixture in the vapor phase reasonably well (Fig. 6) but overestimates the reactivity of nonane compared to heptane. This model predicts a ζ factor of 16.9 (Table 1), much larger than the experimentally observed value of 8.4, which is due to an overestimation of the preference for nonane adsorption. The model illustrates the significance of the interaction term in the Langmuir-with-interaction expression for competitive adsorption.

For the prediction of the liquid-phase conversions, the kinetic parameters from the vapor-phase experiments were used (Table 2). By applying the partition coefficient adsorption model (Eq. [9]) in combination with the rate equations [13]–[16] it was assumed that the composition of adsorbed alkanes in the pores of the zeolite was the same as in the external liquid surrounding the catalyst. The excellent agreement of this catalytic model based on nonselective adsorption with the experimental data can be appreciated in Figs. 5 and 7. The ζ factor according to the model (2.6) is in excellent agreement with the experimental value of 2.7 (Table 1). In liquid-phase catalytic experiments, on a relative basis, the apparent reaction rates correspond to the intrinsic reaction rates.

As expected, the use of the liquid-phase Langmuir adsorption model (Eq. [6]) is inappropriate. It results in a significant overestimation of the nonane conversion rate and underestimation of the conversion rate of heptane (Fig. 5). The average conversion of the mixture is predicted with satisfactory precision (Fig. 6). The Langmuir model results in a ζ factor of 13.9, while the experimental ζ value is 2.7 (Table 1). This clearly demonstrates that the Langmuir isotherm is not suitable in liquid-phase conditions.

In summary, the difference between liquid and vapor phase can be appreciated by plotting the heptane conversion against the nonane conversion (Fig. 8). The suppression of heptane conversion in the vapor-phase conditions is due to the unfavorable adsorption resulting in an abundance of nonane inside the pore, which does not occur when working in the liquid phase.

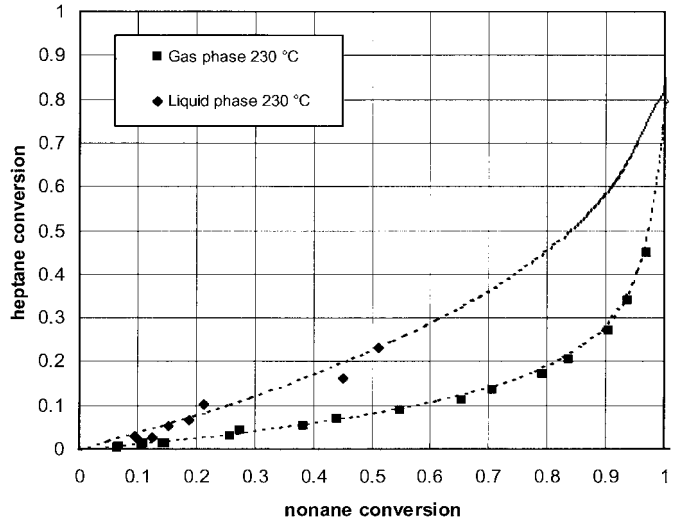

FIG. 8. Comparison between nonane and heptane competition for hydroconversion in vapor and liquid phase on Pt/USY at 230°C: symbols, experimental data; curves, theoretical model.

CONCLUSIONS

In the modeling of hydroconversion of n-alkane mixtures over Pt–USY-type zeolite catalysts, it is indispensable to use appropriate expressions for the multicomponent adsorption equilibria. For vapor-phase conditions resulting in significant pore filling, the Langmuir-with-interaction model is appropriate. Under liquid-phase conditions, a nonselective adsorption model is at stake. Both in vapor- and in liquid-phase reaction conditions, nonane is more reactive than heptane. The reactivity difference is, however, much more pronounced in the vapor phase. In USY zeolite micropores exposed to the vapor of the two n-alkanes, the heaviest alkane molecule is preferentially adsorbed, resulting in a higher apparent reaction rate. When the alkane mixture is fed in the liquid phase, the competing alkanes are adsorbed in a nonselective manner in the micro- and mesopores of USY. Consequently, in liquid-phase conditions the relative reactivity of the n-alkanes corresponds to the relative intrinsic reactivities.

APPENDIX: NOMENCLATURE

$C^{L}_{H_2}$	dissolved hydrogen concentration, mol/m^3
c_i	concentration of component i, mol/m^3
CR	cracked product
K^{vap}_{DH}	dehydrogenation constant in vapor phase, bar
K_i	partition coefficient, m^3/kg
K'_i	Henry constant of component i, mol/(kg bar)
K_{MB}	equilibrium constant between linear and monobranched alkanes
K_{MTB}	equilibrium constant between monobranched and multibranched alkanes

$k_{CR,i}$	rate constant for the conversion of multibranched to cracked alkanes, 1/s
$k_{MB,i}$	rate constant for the conversion of linear into monobranched alkanes, 1/s
$k_{MTB,i}$	rate constant for the conversion of monobranched into multibranched alkanes, 1/s
L_i	Langmuir constant of component i, 1/bar
MB	monobranched alkane
MB O	monobranched olefin
MTB	multibranched alkane
MTB O	multibranched olefin
nA	n-alkane
nO	n-olefin
P	total pressure, bar
p_{H_2}	partial pressure of hydrogen, bar
p_i	partial pressure of component i, bar
q_A	adsorbed amount of alkane, mol/kg
q_i	adsorbed amount of component i, mol/kg
$q_{i,s}$	adsorption capacity of component i, mol/kg
$\bar{q}_s$	average adsorption capacity, mol/kg
q_T	total amount adsorbed, mol/kg
r_i	reaction rate of component i, mol/kg/s
T	temperature, K
V_m	molar volume of the liquid phase, mol/m^3
w_i	adsorption interaction factor

Greek Letters

$\phi^L_{H_2}$	fugacity coefficient of hydrogen in liquid phase

ACKNOWLEDGMENTS

This research was financially supported by FWO Vlaanderen (G.0127.99). J. Denayer is grateful to FWO-Vlaanderen for a fellowship as postdoctoral researcher. The involved teams (Dienst Chemische Ingenieurstechniek, Vrije Universiteit Brussel; Centrum voor Oppervlaktechemie en Katalyse, Katholieke Universiteit Leuven; and Laboratorium voor Petrochemische Techniek, Universiteit Gent) are participating in the IAP-PAI Program on Supramolecular Chemistry and Catalysis, sponsored by the Belgian government.

REFERENCES

1. Maxwell, I. E., and Stork, W. H. J., *Stud. Surf. Sci. Catal.* **137**, 747 (2001).
2. Guisnet, M., *Catal. Today* **1**, 415 (1987).
3. Dauns, H., and Weitkamp, J., *Chem.-Ing.-Tech.* **11**, 900 (1986).
4. Tromp, M., van Bokhoven, J. A., Garriga Oostenbrink, M. T., Bitter, J. H., de Jong, K. P., and Koningsberger, D. C., *J. Catal.* **190**(2), 209 (2000).
5. de Gauw, F. J. M. M., van Grondelle, J., and van Santen, R. A., *J. Catal.* **204**(1), 53 (2001).
6. Denayer, J. F. M., Baron, G. V., Jacobs, P. A., and Martens, J. A., *J. Phys. Chem. B* **102**(17), 307 (1998).
7. Kiselev, A. V., *Adv. Chromatogr.* **4**, 113 (1967).
8. Denayer, J. F. M., and Baron, G. V., *in* "Proc. Fundamentals of Adsorption" (F. Meunier, Ed.), Vol. 6, pp. 99–104. Elsevier, Paris, 1998.
9. Denayer, J. F. M., Bouyermaouen, A., and Baron, G. V., *Ind. Eng. Chem. Res.* **37**(9), 3691 (1998).
10. Muñoz Arroyo, J. A., Thybaut, J. W., Marin, G. B., Martens, J. A., Jacobs, P. A., and Baron, G. V., *J. Catal.* **198**, 29 (2001).
11. Munoz Arroyo, J. A., Martens, G. G., Froment, G. F., Marin, G. B., Jacobs, P. A., and Martens, J. A., *Appl. Catal., A* **192**, 9 (2000).
12. Martens, J. A., Jacobs, P. A., and Weitkamp, J., *Appl. Catal.* **20**, 239 (1986).
13. Martens, J. A., Tielen, M., and Jacobs, P. A., *Catal. Today* **1**, 435 (1987).
14. Coonradt, H. L., and Garwood, W. E., *Ind. Eng. Chem.* **1**, 38 (1964).
15. Denayer, J. F. M., Baron, G. V., and Martens, J. A., *J. Catal.* **190**(2), 469 (2000).
16. Thybaut, J. W., Marin, G. B., Martens, J. A., Jacobs, P. A., and Baron, G. V., *J. Catal.* **202**, 324 (2001).
17. Martens, G. G., Marin, G. B., Martens, J. A., Jacobs, P. A., and Baron, G. V., *J. Catal.* **195**, 253 (2000).
18. Denayer, J. F. M., Baron, G. V., and Martens, J. A., *Phys. Chem. Chem. Phys.* **2**(5), 1007 (2000).
19. Froment, G. F., *Catal. Today* **1**, 455 (1987).
20. Debrabandere, B., and Froment, G. F., *Stud. Surf. Sci. Catal.* **106**, 379 (1997).
21. Ruthven, D. M., "Principles of Adsorption and Adsorption Processes." Wiley, New York, 1984.
22. Martens, G. G., and Marin, G. B., *AIChE J.* **47**(7), 1607 (2001).